Available online at www.sciencedirect.com
SCIENCE DIRECT®
Materials Science and Engineering C 26 (2006) 1251 – 1260
MATERIALS SCIENCE & ENGINEERING C
www.elsevier.com/locate/msec

Role of microstructure in the aging-related deterioration of the toughness of human cortical bone

R.K. Nalla [a], J.J. Kruzic [b], J.H. Kinney [c], M. Balooch [c], J.W. Ager III [a], R.O. Ritchie [a,*]

[a] *Materials Sciences Division, Lawrence Berkeley National Laboratory, and Department of Materials Science and Engineering, University of California, Berkeley, CA 94720, United States*
[b] *Department of Mechanical Engineering, Oregon State University, Corvallis, OR 97331, United States*
[c] *Department of Preventive and Restorative Dental Sciences, University of California, San Francisco, CA 94143, United States*

Available online 3 October 2005

Abstract

The aging-related deterioration of the fracture properties of bone, coupled with higher life expectancy, is responsible for increasing incidence of bone fracture in the elderly; consequently, an understanding of how these fracture properties degrade with age is essential. In this study, ex vivo fracture experiments have been performed to quantitatively assess the effect of age on human cortical bone in the proximal–distal orientation, i.e., longitudinally along the osteons. Because cortical bone exhibits rising crack-growth resistance with crack extension, the toughness is evaluated in terms of resistance-curve (R-curve) behavior, measured for bone taken from wide range of age groups (34–99 years). Using this approach, both the crack-initiation and crack-growth toughness are determined and are found to deteriorate with age; the initiation toughness decreases some 40% over six decades from 40 to 100 years, while the growth toughness is effectively eliminated over the same age range. The reduction in crack-growth toughness is considered to be associated primarily with a degradation in the degree of extrinsic toughening, in particular, involving crack bridging in the wake of the crack. An examination of the micro-/nano-structural changes accompanying the process of aging, using optical microscopy, X-ray tomography, nanoindentation and Raman spectroscopy, is shown to support such observations.
Published by Elsevier B.V.

Keywords: Cortical bone; Aging; Fracture toughness; R-curve; Tomography; Bridging

1. Introduction

There is mounting evidence that the traditional thinking concerning "bone quality", which has largely focused on bone mass or bone mineral density as a predictor of fracture risk, is insufficient [1–3]. This is particularly a concern as aging-related changes to the musculoskeletal system are known to increase the susceptibility to bone fracture [1]; indeed, for the very elderly, the consequent fractures can lead to mortality [4]. This has led to a renewed interest into how aging can alter the various mechanical properties of bone, and in particular the fracture resistance. Specifically, there have been several recent studies that have focused on age-related issues and have shown a significant deterioration in the fracture toughness of bone with age (e.g., [5–13]).

In order to characterize the deterioration of bone with age, generally the fracture toughness, K_c, or the strain-energy release rate, G_c, has been used as a single-parameter approach to characterize the resistance to fracture. However, in many materials, including cortical bone, so-called *extrinsic* toughening mechanisms, such as constrained microcracking or crack bridging [14], are active. In general, crack propagation can be considered as a mutual competition between two classes of mechanisms: *intrinsic* mechanisms that operate ahead of the crack tip, and affect the material's inherent resistance to fracture and damage, and *extrinsic* mechanisms that principally operate in the wake of the crack tip, and "shield" the crack from the applied driving force [15–17]. Whereas intrinsic mechanisms primarily govern the crack-initiation toughness, extrinsic mechanisms, specifically crack bridging in bone [18], operate in the crack wake and govern the crack-growth toughness. As the effect of extrinsic mechanisms is dependent on the size of the crack and stable crack growth can occur prior to unstable fracture, this requires a "resistance-curve" approach

* Corresponding author. Tel.: +1 510 486 5798; fax: +1 510 486 4881.
E-mail address: RORitchie@lbl.gov (R.O. Ritchie).

0928-4931/$ - see front matter. Published by Elsevier B.V.
doi:10.1016/j.msec.2005.08.021

to evaluate the fracture toughness [19]. Despite this, R-curves have only been utilized in relatively few studies [13,14,18,20,21] to characterize human bone fracture.

Mechanistically, it has been suggested that the elevated bone turnover in older bone, although beneficial in repairing damage [22], may have a deleterious effect on the toughness due to the formation of resorption cavities and hence increased porosity. Elevated turnover also results in a higher density of secondary osteons [23], and associated cement lines which are known to provide weak interfaces, and hence preferred (weaker) paths, for cracking [13,24–27]. In the present paper, we seek to investigate the ex vivo R-curve fracture toughness properties of human cortical bone as a function of age, with the aim of elucidating the role that these age-related changes in the microstructure play. Furthermore, we show that the age-related changes in macroscopic properties can be linked to changes of the hierarchical structure of bone at the micro- and nano-scales [28] (Fig. 1). This is achieved specifically at the nanoscale using both nanoindentation, to obtain moduli of the collagen fibers that constitute the osteons, and deep-ultraviolet (UV) Raman spectroscopy, to ascertain corresponding changes in the cross-linking in the collagen.

2. Experimental methods and materials

2.1. Fracture toughness testing

Fresh frozen human cortical bone taken from the humerus of nine cadavers (donor age: 34 to 99 years) was used. Blocks of bone were obtained by carefully sectioning the medial cortices of the mid-diaphyses of the humeri. Seventeen ($N=17$)

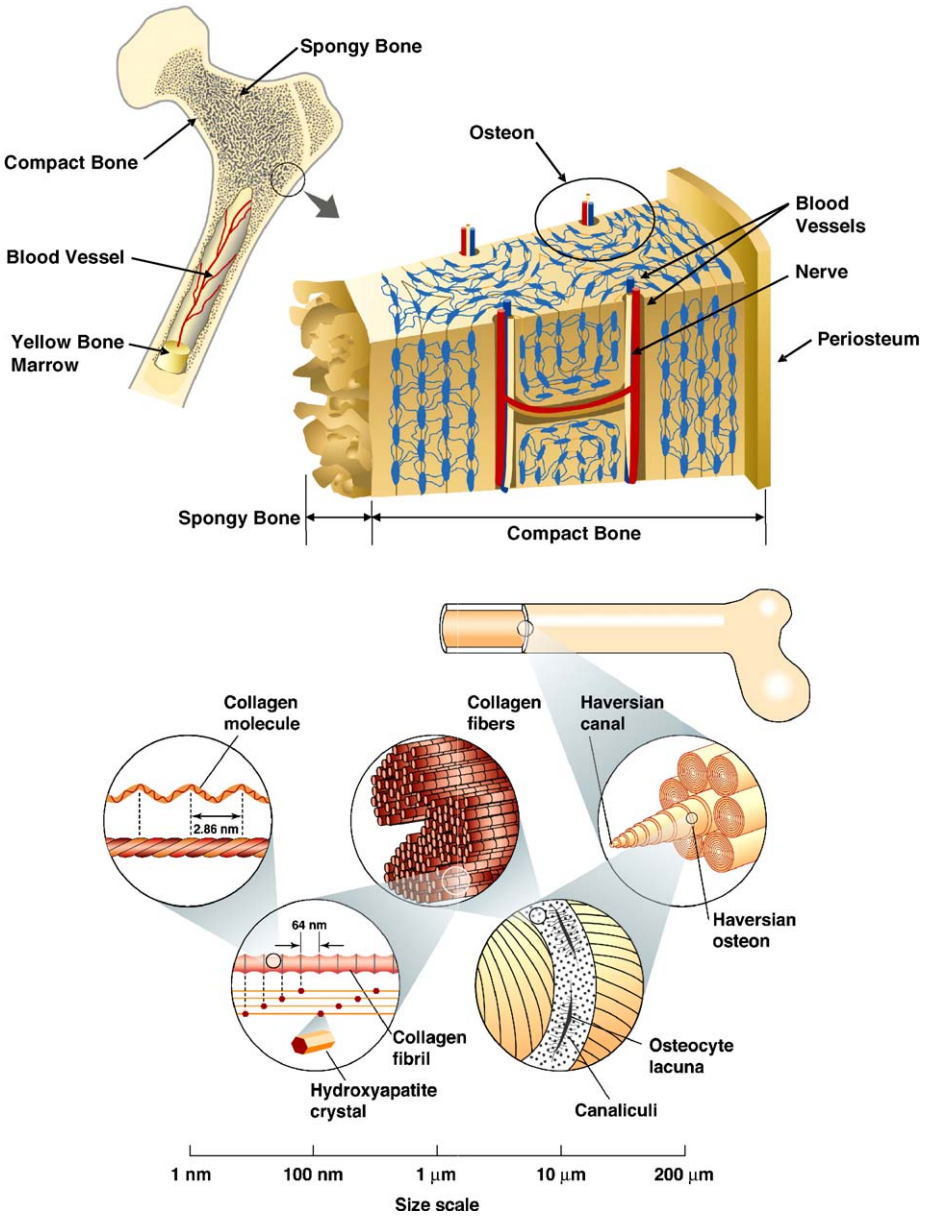

Fig. 1. Hierarchical structure of human cortical/compact bone.

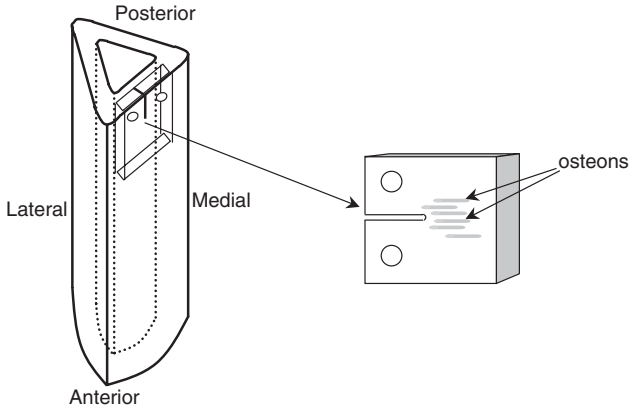

Fig. 2. Schematic showing the anatomical orientation that the compact-tension, C(T), specimens were taken from the humeri to permit crack extension in the proximal–distal direction (nominal orientation with respect to the osteons is also indicated).

compact-tension, C(T), specimens, with specimen thicknesses, $B \sim 1.2–3.3$ mm, widths, $W \sim 13–18.3$ mm and initial crack lengths, $a \sim 3.0–5.5$ mm, were machined from these blocks, and divided into three age groups — arbitrarily named *Young*, *Middle-Aged* and *Aged*:

- *Young*: 34 ($N=1$), 37 ($N=4$) and 41 ($N=2$) years,
- *Middle-Aged*: 61 ($N=1$), 69 ($N=2$) and 69 ($N=2$) years, and
- *Aged*: 85 ($N=1$), 85 ($N=2$) and 99 ($N=2$) years.

The samples were all orientated with the starter notch and the nominal crack-growth direction along the proximal–distal direction of the humerus (in the longitudinal–radial plane), i.e., parallel to the long axis of the osteons and hence, the long axis of the humerus (Fig. 2).

R-curves were measured to evaluate the resistance to fracture in terms of the stress intensity, K, as a function of crack extension, Δa (Fig. 3). The C(T) specimens were thawed and thoroughly hydrated prior to testing by soaking in Hanks' Balanced Salt Solution (HBSS) for at least 40 h at room temperature in air-tight containers. Tests were then conducted in ambient air (25 °C, 20–40% relative humidity) with the specimens being continuously irrigated with HBSS. The specimens were loaded in displacement control using standard servo-hydraulic testing machines (MTS 810, MTS Systems Corporation, Eden Prairie, MN) with a loading rate ~0.015 mm/s until the onset of cracking, which was determined by a drop in load, or non-linearity in the load-displacement curve. At this point, the sample was manually unloaded by 10–20% of the peak load to record the sample load-line compliance at the new crack length using a linear variable-displacement transducer (LVDT) mounted in the load frame. This process was repeated at regular intervals until the end of the test (arbitrarily chosen when data for at least 4 mm of crack growth was obtained), at which point the compliance and loading data were analyzed to determine fracture resistance, K_R, as a function of crack extension, Δa. Crack lengths, a, were calculated from the compliance data obtained during the test using standard C(T) load-line compliance calibrations [29]. Further details of the testing procedures are provided elsewhere [13]. The *crack-initiation toughness*, K_o, was obtained by extrapolating a linear fit of the data for each sample to $\Delta a = 0$, while the (linear) slope of the R-curve gave a measure of the *crack-growth toughness*. Statistical analysis of the data was conducted using the non-parametric Kruskal–

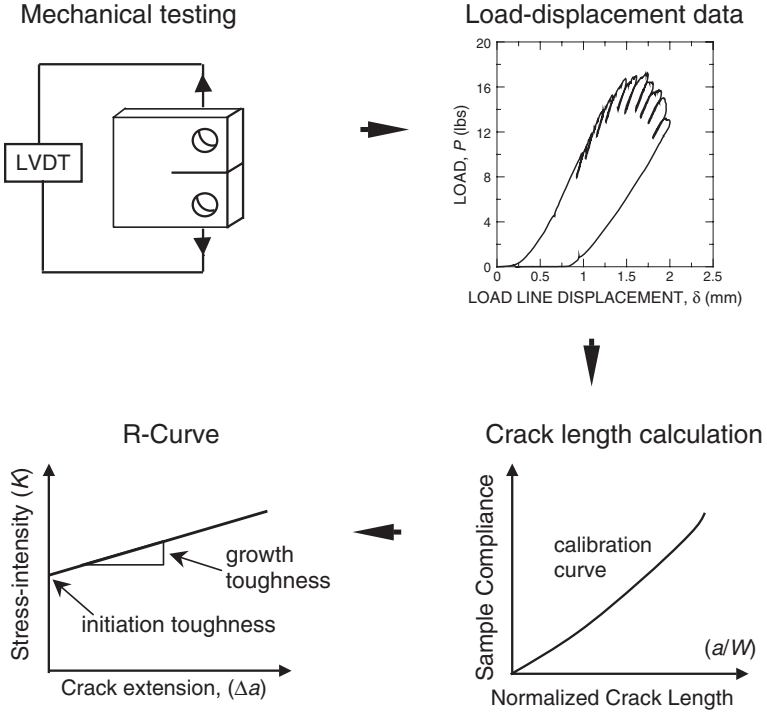

Fig. 3. Schematic illustrating the experimental procedures used in this study to obtain the resistance-curve data.

Wallis test. The data were also subjected to linear regression analysis against age.

2.2. Microstructural examinations

To evaluate the changes in the microstructure during the aging process, cross-sections of the samples were polished and observed under an optical microscope (Olympus STM-UM Measuring Microscope, Olympus America Inc., Melville, NY). Three randomly selected non-intersecting areas measuring 2×1 mm were examined on each specimen and the number of secondary osteons counted; the average areal density of such osteons was then reported. The data were also subjected to linear regression analysis against age and against both measures of the toughness.

To observe crack–microstructure interactions and possible toughening mechanisms in the fractured specimens, in addition to optical microscopy, synchrotron X-ray computed tomography was performed on two specimens each of the *Young* and *Aged* groups. This work was conducted at the Stanford Synchrotron Radiation Laboratory (SSRL), Menlo Park, CA, and at the Advanced Light Source (ALS), Berkeley, CA. Imaging was performed with monochromatic X-rays (25 keV at SSRL and 18 keV at ALS), with a voxel size (spatial resolution) of ~5 μm. The tomography data were reconstructed using a Fourier-filtered back-projection algorithm; further details of this technique are described elsewhere [30,31]. The two-dimensional "slices" of the crack front obtained were examined for evidence, both qualitative and quantitative, of crack bridging.

2.3. Nanoindentation experiments

To evaluate the changes at the collagen fibrillar level, nanoindentation tests were performed on individual collagen fibers in partially decalcified bone samples using an atomic force microscope, AFM (Nanoscope III, Veeco, Santa Barbara, CA), to which a force-displacement transducer (Triboscope Micromechanical Test Instrument, Hysitron Inc., Minneapolis, MN) was attached. The unloading load-displacement data obtained were used to determine the elastic modulus based on classical indentation theory [32]; further details are given elsewhere for similar experiments [33].

2.4. Deep-UV Raman spectroscopy experiments

Deep-UV Raman spectroscopy was used to evaluate age-related changes at a more fundamental level. A 5 mW, 244 nm spot, continuous wave, intracavity doubled, argon ion laser was used, and spectra were collected with a CCD camera. Spectra were then normalized to the CH_2 wag peak height at ~1460 cm^{-1}. The most pronounced changes were found in the amide I band, which is reflective of cross-linking in bone [34]. For specific analysis of this region, non-linear least-squares fitting to four features centered at ~1460 cm^{-1} (CH_2 wag), 1580 cm^{-1} (amide II), 1610 cm^{-1} (amide I), and 1655 cm^{-1} (amide I) was employed.

3. Results

3.1. Resistance curve results

The ex vivo load-displacement data obtained were analyzed to evaluate the resistance to fracture in terms of the stress intensity, K, as a function of crack extension, Δa (Fig. 3). The resulting monotonically rising R-curves are shown in Fig. 4. Mean crack-initiation toughness, K_o, values of 2.07 (S.D.=0.11), 1.96 (S.D.=0.15), and 1.26 (S.D.=0.22) MPa√m, and mean slopes (crack-growth toughness) of 0.37 (S.D.=0.06), 0.16 (S.D.=0.01), and 0.06 (S.D.=0.04) MPa√m/mm were thus obtained for the *Young*, *Middle-Aged*, and *Aged* groups, respectively. Statistical analysis indicated that, for the three age groups, variation among group medians was significant ($p=0.025$ and 0.0036 for the initiation and the growth toughness, respectively). These data are plotted in Fig. 4 as variations of the crack-initiation and growth toughnesses as a function of age. While the initiation toughness decreases with age, the effect of aging is more evident on the growth toughness which is essentially eliminated in the *Aged* group.

3.2. Microstructural examinations

Fig. 5 shows data for the osteonal density in the specimens measured using optical microscopy as a function of the donor age. There is a definitive, highly statistically significant ($p=0.0002$) increase in the areal density of secondary osteons with age; indeed, the density almost doubles over the age range examined. Regressions of the osteonal density against the crack-initiation and growth toughnesses are shown in Fig. 6. Clearly, there is a very significant decrease in both measures of the toughness ($p=0.0031$ and 0.0065 for the crack-initiation and

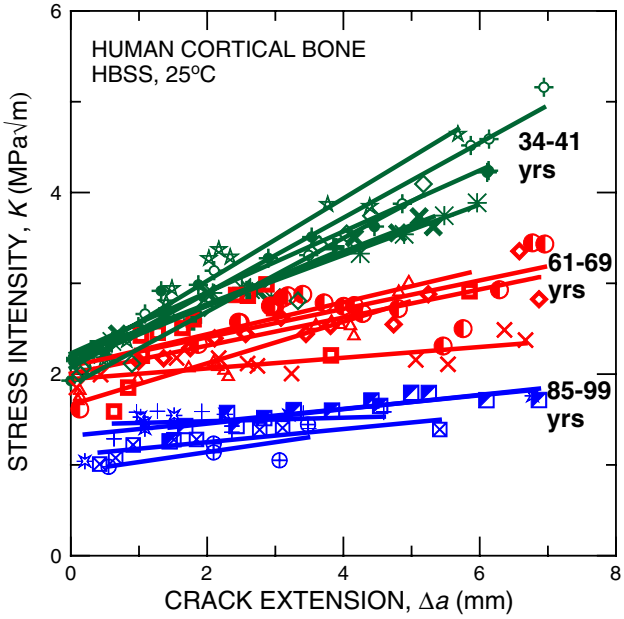

Fig. 4. Resistance-curves for stable ex vivo crack extension in human cortical bone obtained in this study. Note the linearly rising R-curve behavior.

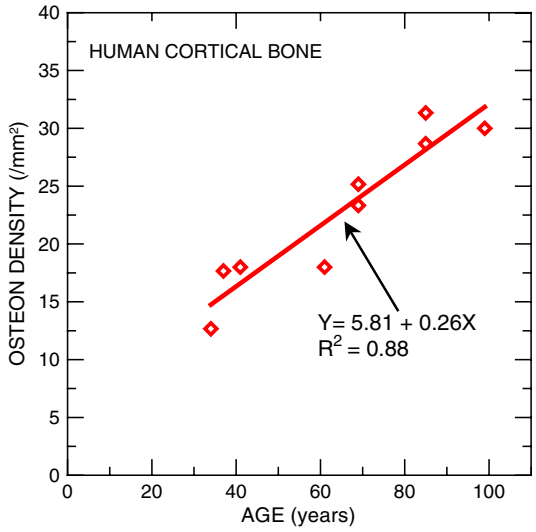

Fig. 5. Variation in the areal density of secondary osteons with age for the human cortical bone used in this study. A linear regression of the data is shown (fit equation and coefficient of determination, R^2, are also included).

growth toughnesses, respectively) with increasing osteonal density.

Optical microscopy of the crack paths revealed evidence of crack bridging in all the specimens (Fig. 7). Such bridging is from the formation of "uncracked ligaments" in the crack wake; these are intact regions, often tens of micrometers in size, that form along the crack path, either by the non-uniform advance of the crack front and/or by the imperfect linking of microcracks, that initiated ahead of the crack tip, with the main crack. This mechanism has been shown to be the primary source of extrinsic toughening for cracking in the longitudinal orientation in bone and is responsible for the rising R-curve behavior [14,18].

Fig. 8a–b shows typical two-dimensional through-thickness "slices" obtained by tomography for specimens belonging to the *Young* and *Aged* groups at various distances behind the crack tip. There is evidence of crack bridging in both cases. Further examination of the tomographic slices revealed that there is a definitive decrease in the size and number of these bridges with age. Fig. 8c shows the variation in the areal fraction of such bridges with distance from the crack tip for *Young* and *Aged* bone. It is apparent that the bridging zones are larger in *Young* bone (roughly 5.5 mm vs. 3.5 mm), and within the zone, the areal fractions are in general larger for that group. The three-dimensional nature of these bridges is also evident from the reconstructed tomography image in Fig. 9. Additionally, these images (optical and tomography) show that the cracks do not actually penetrate the osteon, but take off along the cement lines between osteons, suggesting an important role for the cement line.

3.3. Nanoindentation results

AFM-based indentation of collagen fibers revealed a change in the elastic properties with age. Fig. 10 shows typical AFM images and nanoindentation moduli measured.

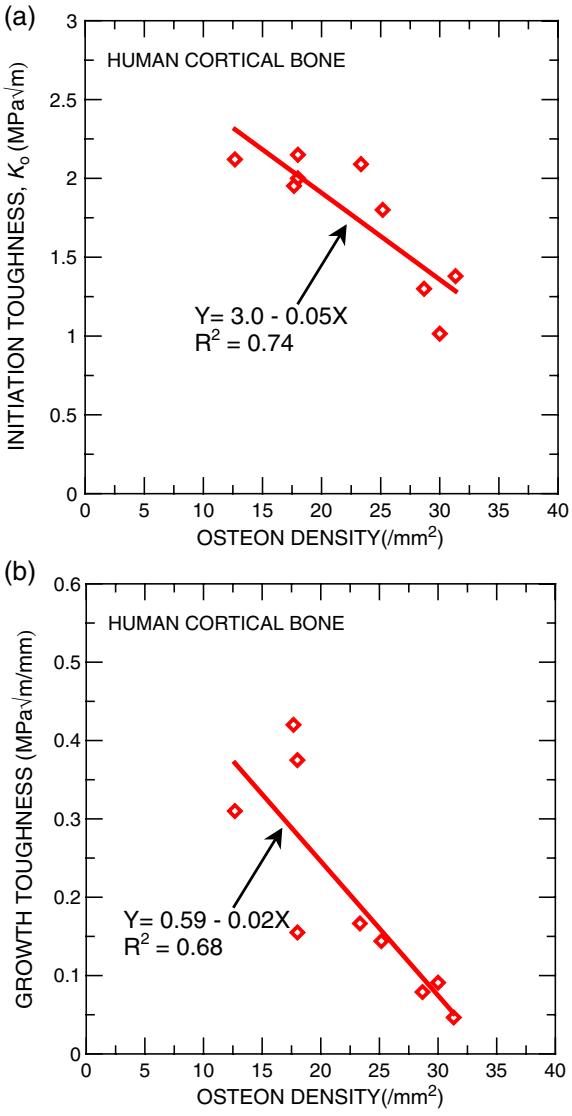

Fig. 6. Variation in the (a) crack-initiation toughness, K_o, and the (b) crack-growth toughness (slope of the R-curve) with osteon density for human cortical bone. Each data point represents the average for all measurements from one donor. A linear regression of the data is shown in each case (fit equation and coefficient of determination, R^2, are also included).

While the collagen in the younger bone showed a very regular structure with well-defined "Hodge–Petruska" banding, this was not always the case in older bone where areas

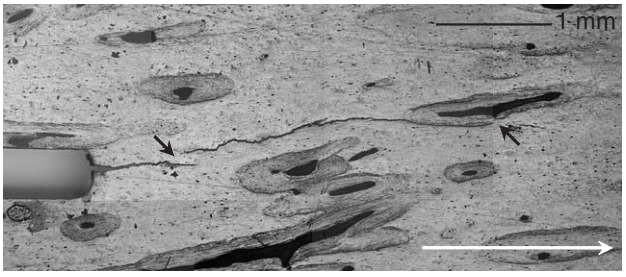

Fig. 7. A typical optical micrograph of stable crack growth in a 34-year old human cortical bone clearly supports the presence of uncracked ligaments (indicated by black arrows) in the crack wake. The white arrow at the bottom gives the direction of nominal crack growth.

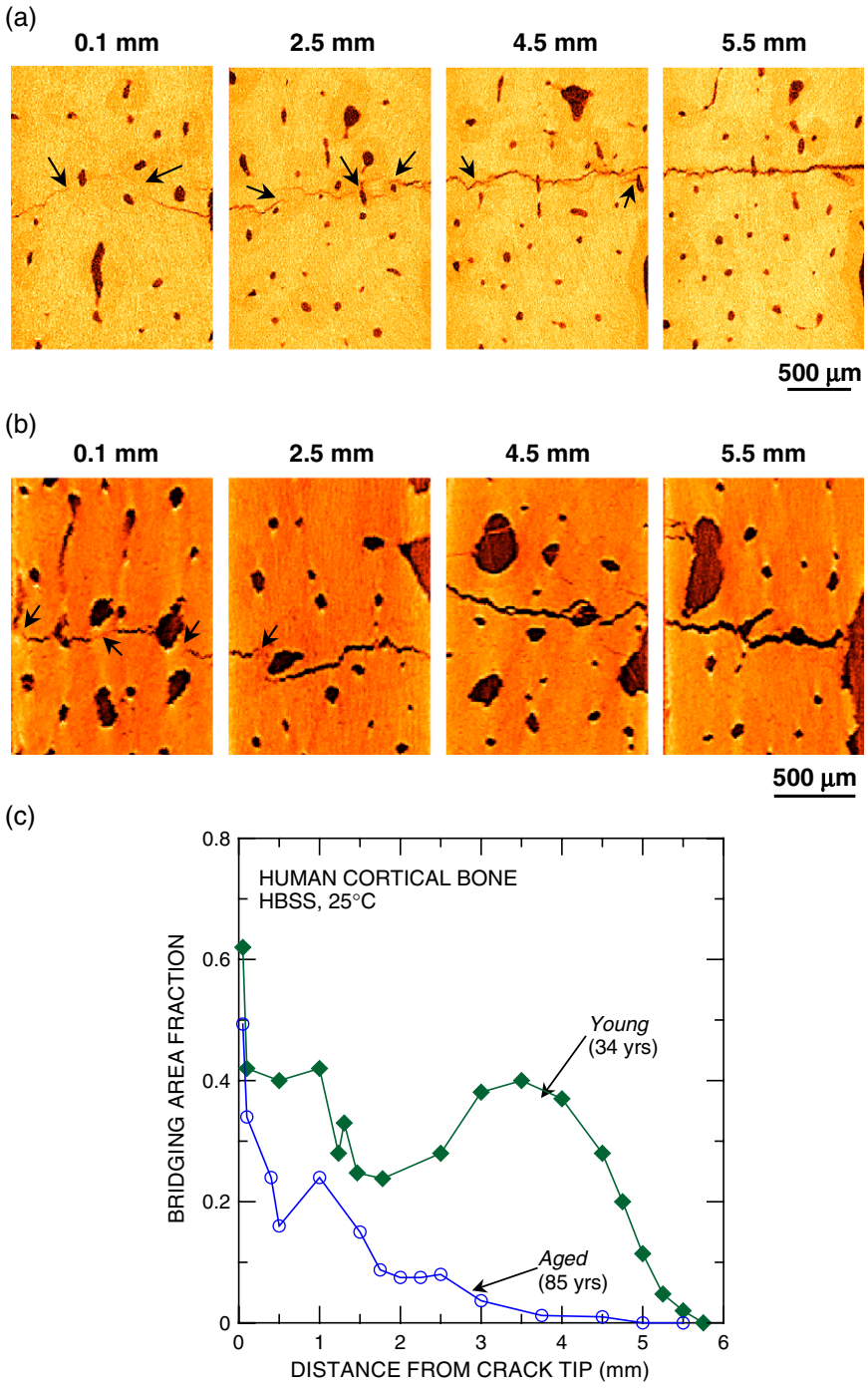

Fig. 8. Two-dimensional computed X-ray tomographic reconstruction slices showing typical cracks in specimens taken from the (a) *Young* (34 years), and (b) *Aged* (85 years) groups. The numbers on top of each figure indicate the distance from the (nominal) crack tip, and the black arrows indicate the presence of "uncracked-ligament" crack bridges. The smaller porosity are the Haversian canals in cross-section, while the much larger porosity seen particularly in the older bone are partially filled resorption cavities. (c) The fraction of such bridges with distance from the crack tip indicating smaller areal fractions and bridging-zone size in the older bone. Note that slices in (a) and (b) are not at the same magnification.

with relatively disorganized collagen with lower moduli were often encountered. More extensive evaluations are currently being undertaken.

3.4. Raman spectroscopy results

Fig. 11 shows deep-UV Raman data in the organic portion of the spectrum (~1400–1800 cm^{-1}) for representative specimens. Three organic bands are strongly resonance enhanced and definitively identified — amide III (primarily from the in-phase combination of NH in-plane bend and CN stretch, ~1245–1260 cm^{-1}), CH_2 wag (~1454–1461 cm^{-1}) and amide I (primarily from the C═O stretch, ~1626–1656 cm^{-1}). The amide II band (primarily from the out-of-phase combination of NH in-plane bend and CN stretch) that is sometimes seen in IR spectra at ~1540–1580 cm^{-1} [35] was rather weak, presumably as it was

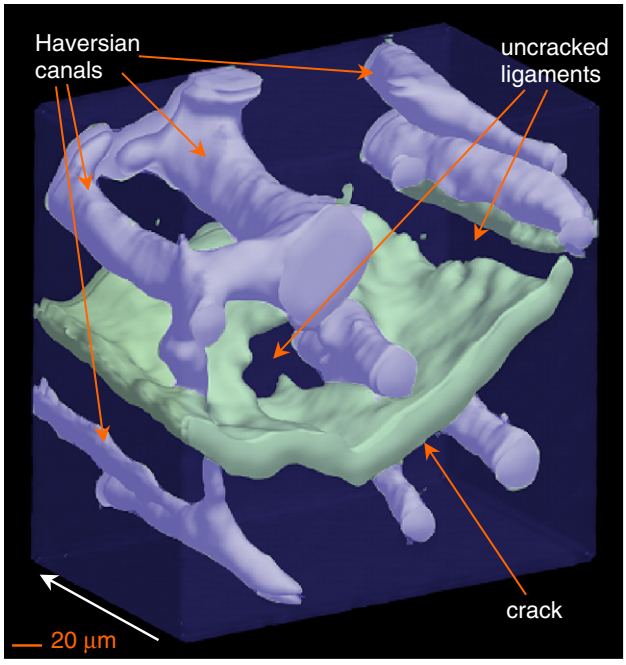

Fig. 9. Three-dimensional tomographic reconstructions of sections of the crack in a 34-year old human cortical bone are shown. Note that the crack appears to follow the cement lines bordering the osteons and does not penetrate the osteon itself. Uncracked ligaments are indicated. The white arrow at the bottom is the direction of nominal crack growth.

not as strongly resonance enhanced. Large changes in peak shape were observed for the amide I band, particularly in the spectra from the very elderly donors (85–99 years). The changes in band shape were made more quantitative by fitting the amide I region to overlapping Gaussian peaks (Fig. 11). The ratio of the areas of the major peaks used for the fits, 1610/1655 cm^{-1}, showed good correlation with age. The amide bands, particularly amide I and amide III, are believed to be good indicators of protein conformation because of the role of the amide moiety in cross-linking and bonding [36]. Paschalis et al. [34] have deconvoluted FTIR spectroscopic data into overlapping component peaks to probe the secondary structures in bone collagen and reported that peaks at ~1660 and 1690 cm^{-1} underlying the amide I band are particularly indicative of the cross-linking, with the area ratio between them (1660/1690) corresponding to the non-reducible/reducible cross-link ratio. This ratio was observed to increase with age in demineralized bovine bone. Our data did not reveal an underlying peak at ~1690 cm^{-1}; this component of the amide I band is not resonance enhanced. However, we did observe an aging-induced increase in the contribution of a peak at ~1655 cm^{-1}, consistent with an increase in the non-reducible (Pyr) cross-link content in bone. These results imply that the protein conformation in the organic matrix (~90–95% collagen) does indeed change with age. More detailed studies with appropriate purified peptide standards are currently underway to quantify such changes.

4. Discussion

The R-curve data are plotted in Fig. 12 as variations of the crack-initiation and growth toughnesses as a function of age. The only other age-related R-curve data available for human cortical bone, from Vashishth et al. [20] and from Wu and Vashishth [21], are also included for the purpose of comparison. While the initiation toughness data from these studies agrees well with the trend suggested by the linear regressions in Fig. 12, there is a stronger effect of age on the growth toughness in Ref. [21] as compared to our data. It should be noted that the bone used in those studies was from a different anatomical location (tibia in Ref. [20] and femur in Ref. [21]). There is a clear, observable trend of decreasing toughness with age in the present study; specifically, the crack-initiation toughness decreases by ~40% over six decades from 40 to 100 years, while the growth toughness is essentially eliminated over the same age range. Such deterioration in the fracture resistance with age is consistent with the trend observed in studies that report single-value toughnesses (e.g., [5–12,37–41]). What is important about these results, together with those of Wu and Vashishth [21], is that they clearly show that not only the

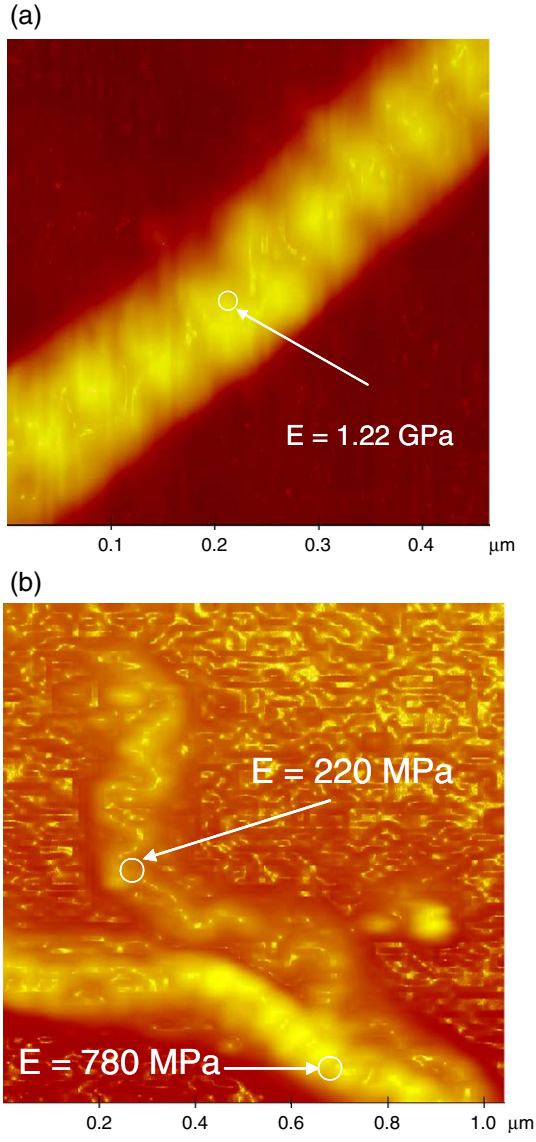

Fig. 10. AFM images with nanoindentation moduli for collagen fibers from (a) Young (37 years), and (b) Aged (99 years) groups.

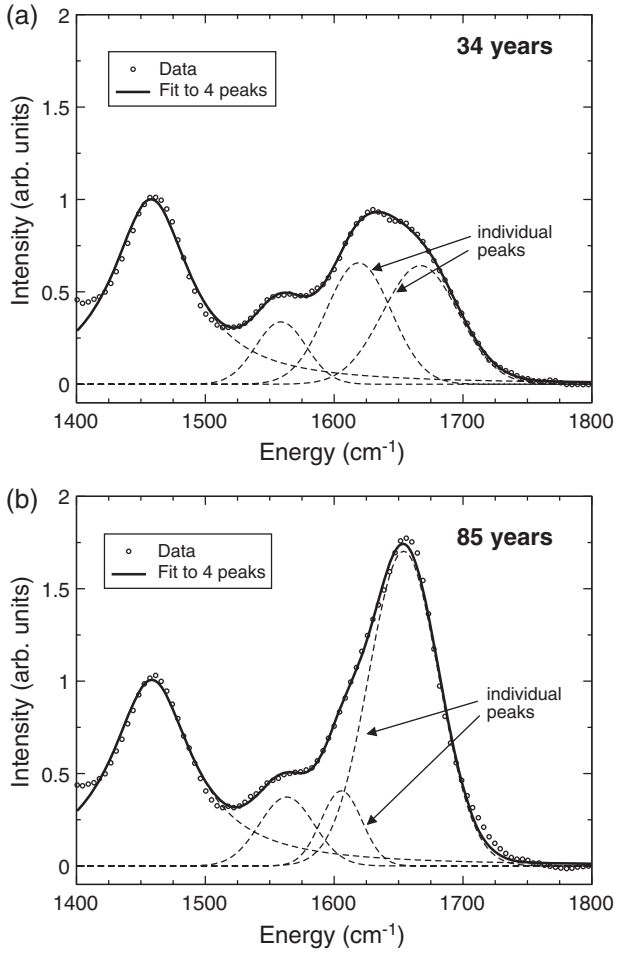

Fig. 11. UV Raman data for bone from (a) Young (34 years), and (b) Aged (85 years) groups. Details of the peak fitting to the CH_2 wag and amide I region are also included.

intrinsic resistance to fracture (as reflected by the crack-initiation toughness), but also the resistance to crack propagation (as reflected by the crack-growth toughness) decreases with age (Fig. 12). Indeed, the age-related deterioration in the crack-growth toughness is clearly the more dominant effect.

Our results show a definitive increase in the areal density of secondary osteons in older bone (Fig. 5), implying that there is an increase in the incidence of smaller osteons with aging; this is to be expected as more extensive remodeling occurs in older bone to repair damage. The corresponding increase in the density of cement lines implies an increased proportion of "weaker paths" in the microstructure of older bone. This would permit easier crack initiation, and hence lower the initiation toughness, consistent with our observations (Fig. 6a). Furthermore, based on crack–microstructure interaction observations, we believe that crack growth in bone in this orientation occurs when the cement line fails ahead of the advancing crack, and the resulting microcrack links back up with the main crack through the intervening tissue. This process of linking up would keep the advancing crack tip sharp and would also support the formation of crack bridges in the wake of the crack where full coalescence with the main crack has not been achieved. Such a mechanism would imply that the smaller osteon size in older bone (reflected by the increase in the areal density of secondary osteons in Fig. 5) would lead to smaller bridges. Conversely, it is plausible that the higher areal density of cement lines could imply easier bridge formation in older bone. Our observations revealed that, overall, the areal fraction of bridges and the extent of the bridging zone in older bone was significantly lower (Fig. 8).

As noted previously, the crack-growth toughness is reflective of the contribution from extrinsic toughening mechanisms, which in bone are principally associated with crack bridging [18]. The prime source of such bridging in human

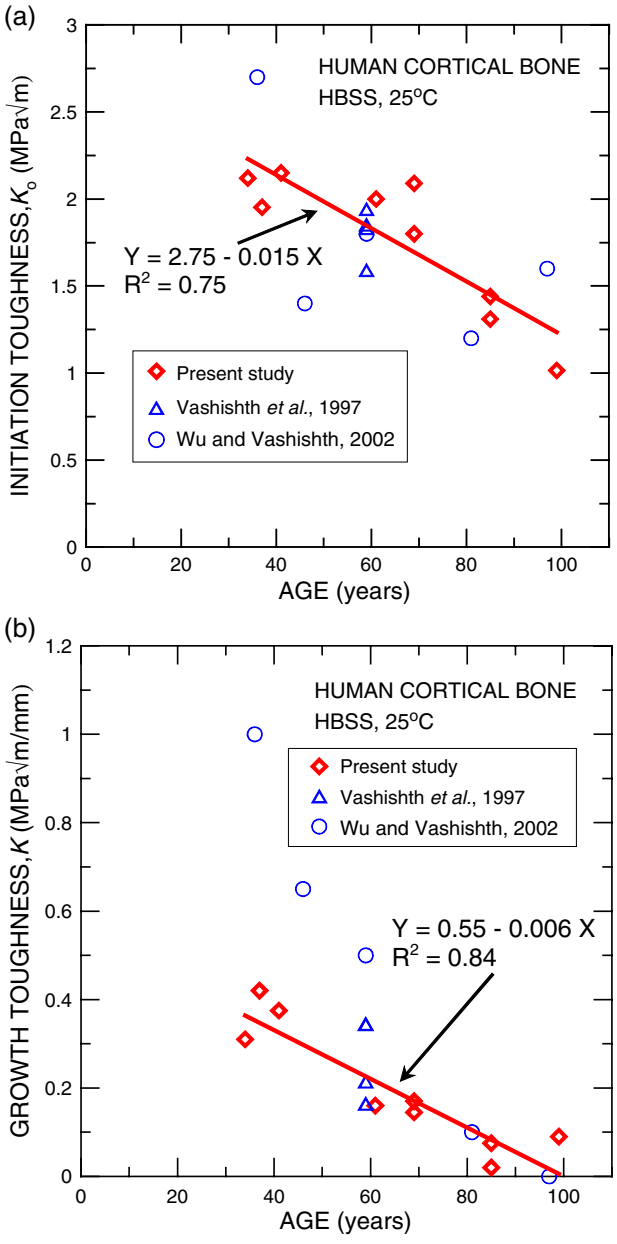

Fig. 12. Variation in the (a) crack-initiation toughness, K_o, and the (b) crack-growth toughness (slope of the R-curve) with age for human cortical bone. Each data point represents the average for all measurements from one donor. A linear regression of the data is shown in each case (fit equation and coefficient of determination, R^2, are also included). Data from Vashishth et al. [20] and Wu and Vashishth [21] are also plotted for comparison (not included in regression).

bone appears to be from the formation of uncracked ligaments in the crack wake. The results in Figs. 8, 12 strongly imply that the contribution from such a mechanism is markedly reduced with age. The magnitude of this contribution is dictated by the size of the bridging zone, the areal fraction of the bridges in the zone, and their load-bearing capacity. All of these factors may change with aging; indeed, Fig. 8c shows that there is a lower density of such bridges in older bone, consistent with the observed reduction in crack-growth toughness (Fig. 12b).

The many effects of aging have been studied on the micro- and ultra-structure of bone, i.e., at micro- and nano-scale dimensions, induced by such factors as increased mineralization [42], increased microdamage [43], lowered collagen quality [40], and increased bone turnover [23]; despite this, the underlying mechanisms that result in age-related changes in fracture resistance remain poorly understood. Increased mineralization has been implicated in reduced elastic deformability [12] and toughness [41]. Increased levels of microdamage (microcracking) have also been shown to lower the fracture resistance [44], presumably by lowering the intrinsic toughness. Possible changes in collagen network integrity with age [40] could result in weaker bridges, and, hence, a lower crack-growth toughness in older bone. Our nanoindentation results directly support the notion of a deterioration in the mechanical properties at the collagen level (Fig. 10). More specifically, age is known to increase non-enzymatic cross-linking in the collagen [40]; as this reduces the post-yield deformation of the collagen, this also has been used to explain the age-induced reduction in growth toughness via a microcracking model [20], although recent studies have cast doubt on the significance of microcracking in beneficially affecting the toughness of bone [14,18]. Our spectroscopy results also support a change in the cross-linking with age (Fig. 11); however, at this stage, it is unclear how such cross-linking actually relates to the deterioration in macroscopic fracture properties.

Finally, it has been suggested that elevated bone turnover in older bone [22], though beneficial in repairing damage, may have a deleterious effect on the toughness due to the formation of resorption cavities and hence increased porosity. Elevated turnover also results in a higher density of secondary osteons [23], and associated cement lines which are known to provide weak interfaces, and hence preferred (weaker) paths, for cracking [18,24–26,45], consistent with the present observations. In fact, a recent study has concluded that elevated turnover is a risk factor in its own right, independent of its actions on bone mineral density [3].

Thus, although the age-induced decrease in the fracture toughness of bone has been clearly quantified, specifically in terms of resistance to both crack initiation and more importantly crack growth, the mechanistic reasons for this deterioration are as yet unclear. As the microstructural factors affecting crack initiation and growth in most materials are invariably quite distinct [15–17], the challenge is to identify *and quantify* the specific mechanisms affecting each process in terms of the changes that occur in the micro/ultra-structure of bone with age.

5. Summary and conclusions

In summary, the fracture toughness of cortical bone, expressed in terms of rising R-curve behavior, shows significant deterioration with aging. In quantitative terms, the ex vivo crack-initiation toughness was reduced by ~40%, whereas the crack-growth toughness was effectively eliminated, as age increased from 34 to 99 years. These results demonstrate the need to interpret this deterioration in bone quality in terms of specific age-related changes in the microstructure of bone that separately affect the crack initiation and growth stages of fracture, both for the purpose of fully characterizing the aging properties of bone and for identifying the actual mechanisms that ultimately increase its fragility and fracture susceptibility. In this regard, the present results have clearly identified that a primary mechanistic factor in the deterioration in the toughness of bone with age can be associated with a degradation in the crack bridging at the microstructural level that is developed in the crack wake. We relate such phenomena to an increase in the density of secondary osteons with age, which we believe is responsible for the observed decrease in both the crack-initiation toughness (due to a higher fraction of weaker cement lines) and crack-growth toughness (due to the formation of small bridges). We have also observed diminished properties and changes in the cross-linking in the collagen at the nanoscale level. Such an investigation helps form the basis of a micromechanistic framework for understanding mineralized tissue fracture and failure in the context of aging and, ultimately, in developing therapies to counter the deleterious effects of the aging process.

Acknowledgements

This work was supported by the National Institutes of Health under Grant No. 5R01 DE015633 (for RKN), and by the Director, Office of Science, Office of Basic Energy Science, Division of Materials Sciences and Engineering, Department of Energy under contract No. DE-AC02-05CH11231 (for ROR). We acknowledge the support of X-ray wiggler beamline (BL 10-2) at the Stanford Synchrotron Radiation Laboratory (SSRL), supported by Department of Energy contract No. DE-AC02-05CH11231, and the dedicated tomography beamline (BL 8.3.2) at the Advanced Light Source (ALS), supported by the Department of Energy (BES) under contract No. DE-AC02-05CH11231. Finally, we also wish to thank Dr. A. P. Tomsia for his support and Drs. C. Puttlitz and Z. Xu for supply of cortical bone.

References

[1] S.L. Hui, C.W. Slemenda, C.C. Johnston, J. Clin. Invest. 81 (1988) 1804.
[2] T.J. Aspray, A. Prentice, T.J. Cole, Y. Sawo, J. Reeve, R.M. Francis, J. Bone Miner. Res. 11 (1996) 1019.
[3] R. Heaney, Bone 33 (2003) 457.
[4] A.G. Jennings, P. de Boer, Injury 30 (1999) 169.
[5] P. Zioupos, J.D. Currey, Bone 22 (1998) 57.
[6] A. Burstein, D. Reilly, M. Martens, J. Bone Jt. Surg. 58A (1976) 82.
[7] J.D. Currey, J. Biomech. 12 (1979) 459.

[8] Y.N. Yeni, T.L. Norman, Bone 26 (2000) 499.
[9] C.U. Brown, T.L. Norman, Adv. Bioeng. 31 (1995) 121.
[10] W. Bonfield, J.C. Behiri, C. Charalamides, in: E. Schneider (Ed.), Biomechanics: Current Interdisciplinary Research, Martinum Nijhoff Publishers, Dordrecht, 1985.
[11] X.D. Wang, N.S. Masilamani, J.D. Mabrey, M.E. Alder, C.M. Agrawal, Bone 23 (1998) 67.
[12] O. Akkus, F. Adar, M.B. Schaffler, Bone 34 (2004) 443.
[13] R.K. Nalla, J.J. Kruzic, J.H. Kinney, R.O. Ritchie, Bone 35 (2004) 1240.
[14] R.K. Nalla, J.J. Kruzic, R.O. Ritchie, Bone 34 (2004) 790.
[15] R.O. Ritchie, Mater. Sci. Eng. 103 (1988) 15.
[16] R.O. Ritchie, Int. J. Fract. 100 (1999) 55.
[17] A.G. Evans, J. Am. Ceram. Soc. 73 (1990) 187.
[18] R.K. Nalla, J.J. Kruzic, J.H. Kinney, R.O. Ritchie, Biomaterials 26 (2005) 217.
[19] B.R. Lawn, J. Am. Ceram. Soc. 66 (1983) 83.
[20] D. Vashishth, J.C. Behiri, W. Bonfield, J. Biomech. 30 (1997) 763.
[21] P.-C. Wu, D. Vashishth, 2nd Joint EMBS/BMES Conference, IEEE, Houston, TX, 2002.
[22] T.C. Lee, A. Staines, D. Taylor, J. Anat. 201 (2002) 437.
[23] R.W. McCalden, J.A. McGeough, M.B. Barker, C.M. Court-Brown, J. Bone Jt. Surg., Am. Vol. 75 (1993) 1193.
[24] J.C. Behiri, W. Bonfield, J. Biomech. 22 (1989) 863.
[25] Y.N. Yeni, T.L. Norman, J. Biomed. Mater. Res. 51 (2000) 504.
[26] D. Taylor, in: I. Milne, R.O. Ritchie, B.L. Karihaloo (Eds.), Comprehensive Structural Integrity: Fracture of Materials from Nano to Macro, vol. 9, Elsevier Inc., Oxford, U.K., 2003, p. 35.
[27] R.K. Nalla, J.H. Kinney, R.O. Ritchie, Biomaterials 24 (2003) 3955.
[28] J.-Y. Rho, L. Kuhn-Spearing, P. Zioupos, Med. Eng. Phys. 20 (1998) 92.
[29] A. Saxena, S.J. Hudak Jr., Int. J. Fract. 14 (1978) 453.
[30] J.H. Kinney, M.C. Nichols, Annu. Rev. Mater. Sci. 22 (1992) 121.
[31] J.H. Kinney, D.L. Haupt, M.C. Nichols, T.M. Breunig, G.W. Marshall, S.J. Marshall, Nucl. Instrum. Methods Phys. Res., Sect. A, Accel. Spectrom. Detect. Assoc. Equip. 347 (1994) 480.
[32] G.M. Pharr, W.C. Oliver, F.R. Brotzen, J. Mater. Res. 7 (1992) 613.
[33] R.K. Nalla, M. Balooch, J.W. Ager III, J.J. Kruzic, J.H. Kinney, R.O. Ritchie, Acta Biomater. 1 (2005) 31.
[34] E.P. Paschalis, K. Verdelis, S.B. Doty, A.L. Boskey, R. Mendelsohn, M. Yamauchi, J. Bone Miner. Res. 16 (2001) 1821.
[35] A. Carden, M.D. Morris, J. Biomed. Opt. 5 (2000) 259.
[36] J. Bandekar, Biochim. Biophys. Acta 1120 (1992) 123.
[37] C.U. Brown, Y.N. Yeni, T.L. Norman, J. Biomed. Mater. Res. 49 (2000) 380.
[38] J.B. Phelps, G.B. Hubbard, X. Wang, C.M. Agrawal, J. Biomed. Mater. Res. 51 (2000) 735.
[39] P. Zioupos, J.D. Currey, A.J. Hamer, J. Biomed. Mater. Res. 2 (1999) 108.
[40] X. Wang, X. Shen, X. Li, C.M. Agrawal, Bone 31 (2002) 1.
[41] J.D. Currey, K. Brear, P. Zioupos, J. Biomech. 29 (1996) 257.
[42] O. Akkus, A. Polyakova-Akkus, F. Adar, M.B. Schaffler, J. Bone Miner. Res. 18 (2003) 1012.
[43] M.B. Schaffler, K. Choi, C. Milgrom, Bone 17 (1995) 521.
[44] Y.N. Yeni, D.P. Fyhrie, Bone 30 (2002) 509.
[45] R.K. Nalla, J.H. Kinney, R.O. Ritchie, Nat. Mater. 2 (2003) 164.